



**Interannual variability of isotopic composition in water vapor over West Africa**

A. Okazaki et al.

# Interannual variability of isotopic composition in water vapor over West Africa and its relation to ENSO

**A. Okazaki<sup>1</sup>, Y. Satoh<sup>1</sup>, G. Tremoy<sup>2</sup>, F. Vimeux<sup>2,3</sup>, R. Scheepmaker<sup>4</sup>, and K. Yoshimura<sup>1,5</sup>**

<sup>1</sup>Institute of Industrial Science, University of Tokyo, Tokyo, Japan

<sup>2</sup>Laboratoire des Sciences du Climat et de l'Environnement, UMR8212, Institut Pierre Simon Laplace, CEA-CNRS-UVSQ, Gif-sur-Yvette, France

<sup>3</sup>Laboratoire HydroSciences Montpellier, UMR 5569, Institut de Recherche pour le Développement, CNRS-IRD-UM1-UM2, Montpellier, France

<sup>4</sup>SRON Netherlands Institute for Space Research, Utrecht, the Netherlands

<sup>5</sup>Atmosphere and Ocean Research Institute, University of Tokyo, Kashiwa, Japan

Received: 27 May 2014 – Accepted: 25 August 2014 – Published: 22 September 2014

Correspondence to: A. Okazaki (okazaki@rainbow.iis.u-tokyo.ac.jp)

Published by Copernicus Publications on behalf of the European Geosciences Union.

Title Page

Abstract

Introduction

Conclusions

References

Tables

Figures

◀

▶

◀

▶

Back

Close

Full Screen / Esc

Printer-friendly Version

Interactive Discussion



## Abstract

This study was performed to examine the relationship between isotopic composition in near-surface vapor ( $\delta^{18}\text{O}_v$ ) over West Africa during the monsoon season and El Niño–Southern Oscillation (ENSO) activity using the Isotope-incorporated Global Spectral Model. The model was evaluated using a satellite and in situ observations at intraseasonal to interannual timescales. The model provided an accurate simulation of the spatial pattern and seasonal and interannual variations of isotopic composition in column and surface vapor and precipitation over West Africa. Encouraged by this result, a simulation stretching 34 years (1979–2012) was conducted to investigate the relation between atmospheric environment and isotopic signature at the interannual time scale. The simulation indicated that the depletion in the monsoon season does not appear every year at Niamey. The major difference between the composite fields with and without depletion was in the amount of precipitation in the upstream area of Niamey. As the interannual variation of the precipitation amount is influenced by the ENSO, we regressed the monsoon season averaged  $\delta^{18}\text{O}_v$  from the model and annually averaged NINO3 index, and found a statistically significant correlation ( $R = 0.56$ ,  $P < 0.01$ ) at Niamey. This relation suggests that there is a possibility of reconstructing past West African monsoon activity and ENSO using climate proxies.

## 1 Introduction

The El Niño–Southern Oscillation (ENSO) is the strongest mode of interannual variability in the tropics (Dai et al., 1997) and plays an important role in variability of precipitation, temperature, and circulation patterns on this timescale. El Niño can cause catastrophic floods and droughts (Philander, 1983) and damage to ecosystems (Aronson et al., 2000). A recent study projected an increase in the frequency of extreme El Niño events due to global warming (Cai et al., 2014). Therefore, it is essential to understand the natural variability of ENSO. Stable water isotopes ( $\text{D}$ ,  $^{18}\text{O}$ ) have been used

ACPD

14, 24441–24474, 2014

### Interannual variability of isotopic composition in water vapor over West Africa

A. Okazaki et al.

Title Page

Abstract

Introduction

Conclusions

References

Tables

Figures

◀

▶

◀

▶

Back

Close

Full Screen / Esc

Printer-friendly Version

Interactive Discussion



to infer past and present climate since the work of Dansgaard (1964). Several studies have linked ENSO with isotopic variation in precipitation or in seawater under the present climate (e.g., Schmidt et al., 2007; Yoshimura et al., 2008; Tindall et al., 2009). For example, tropical South America (Vuille and Werner, 2005), Western and Central Pacific (Brown et al., 2006), and the Asian monsoon region (Ishizaki et al., 2012) are identified as having a connection with ENSO, basically through changes in local rainfall or integrated rainfall along the trajectory. However, other regions, such as West Africa, have not yet been investigated in detail.

West Africa receives most precipitation in the monsoon season (July–September; JAS) and is known for its high variability at interannual or longer timescales. The severe drought that hit West Africa during the 1970s and 1980s prompted researchers to study the factors controlling West African rainfall variability at interannual to multi-decadal timescales (e.g., Folland et al., 1986; Palmer, 1986; Janicot et al., 1996; Giannini et al., 2003; Shanahan et al., 2009; Mohino et al., 2011a, b). At present, the major role of sea surface temperatures (SST) in driving the variability with land–atmosphere interactions as an amplifier (Giannini et al., 2003) is widely recognized. However, there is still debate regarding the relative importance of the various basins and mechanistic timescales involved (Nicholson, 2013). The Atlantic (Lamb, 1978; Joly and Voldoire, 2010; Mohino et al., 2011a), Pacific (Janicot et al., 2001; Mohino et al., 2011b), Indian Ocean (Palmer et al., 1986), and Mediterranean (Rowell, 2003; Polo et al., 2008) are all candidates. Among them, the ENSO is thought to modulate the high-frequency component (interannual) of the variability (Ward, 1998; Joly et al., 2007). However, the relationships are not stationary over time; the West African rainfall is correlated with ENSO only after the 1970s (Janicot et al., 2001; Losada et al., 2012), indicating the existence of multiple competing physical mechanisms. How the impact has changed remains an open question.

Several studies used isotopes to understand the water cycle over West Africa at the intraseasonal timescale. Risi et al. (2008b) and Tremoy et al. (2012, 2014) examined the isotopic compositions of precipitation ( $\delta^{18}\text{O}_\text{P}$ ) and vapor ( $\delta^{18}\text{O}_\text{V}$ ), respectively, and

## Interannual variability of isotopic composition in water vapor over West Africa

A. Okazaki et al.

Title Page

Abstract

Introduction

Conclusions

References

Tables

Figures

◀

▶

◀

▶

Back

Close

Full Screen / Esc

Printer-friendly Version

Interactive Discussion

# Interannual variability of isotopic composition in water vapor over West Africa

A. Okazaki et al.

Title Page

Abstract

Introduction

Conclusions

References

Tables

Figures

◀

▶

◀

▶

Back

Close

Full Screen / Esc

Printer-friendly Version

Interactive Discussion



both found that  $\delta^{18}\text{O}$  records the spatially and temporally integrated convective activity during the monsoon season. Risi et al. (2010) confirmed the relation using the LMDZ-iso model and suggested that  $\delta^{18}\text{O}$  is controlled by convection through rain re-evaporation and the progressive depletion of the vapor by convective mixing along air mass trajectories. The relation between  $\delta^{18}\text{O}$  and convective activity suggests the possibility of reconstructing the convective activity using a climate proxy, if the relation holds at the interannual timescale. The long record of precipitation should help in determining how SSTs influence precipitation variability.

In this paper, we explore the factors governing the interannual variability of monsoon season  $\delta^{18}\text{O}_v$ , which is the source of precipitation and controls  $\delta^{18}\text{O}_p$  variability (Risi et al., 2008a), over West Africa and how the ENSO signal is imprinted. As the observations cover relatively short periods, we use an isotope-enabled general circulation model (GCM).

In the following section, the model simulations and the observations are described. In Sect. 3, we compare the simulated and observed variability of  $\delta^{18}\text{O}$ . Section 4 investigates the factors controlling  $\delta^{18}\text{O}_v$  at the interannual timescale based on the simulation results. Finally, we examine the relation between  $\delta^{18}\text{O}$  and ENSO in Sect. 5.

## 2 Data and methods

### 2.1 Observations

#### 2.1.1 Observation of HDO in vapor from space

Frankenberg et al. (2009) measured column-averaged isotopologue ratio ( $\delta\text{D}$ ) values in water vapor using the SCanning Imaging Absorption spectroMeter for Atmospheric CHartographY (SCIAMACHY) onboard the European research satellite ENVISAT. We used the updated and extended version of this dataset from Scheepmaker et al. (2014), covering the years 2003–2007. As measured  $\delta\text{D}$  is weighted by the  $\text{H}_2\text{O}$  concentration

at all heights, it is largely determined by the isotopic abundance in the lowest tropospheric layers, where most water vapor resides. The footprint of each measurement is 120 km (across-track)  $\times$  30 km (along-track). We apply the following selection criteria concerning the retrievals (Scheepmaker et al., 2014):

- retrieved H<sub>2</sub>O total column must be at least 70 % of the a priori value.
- The CH<sub>4</sub> column in the same retrieval window must be at least within 10 % of the a priori value.
- Root-mean-square variation of the spectral residuals must be below 5 %.
- Convergence achieved in a maximum of four iteration steps.

Here, the first two criteria restrict large deviations from the a priori H<sub>2</sub>O and CH<sub>4</sub> columns, which are normally the result of light scattering by clouds. Therefore, these two criteria function as a simple cloud filter. Due to high detector noise of SCIAMACHY in the short-wave infrared channels, the single measurement noise ( $1\sigma$ ) is typically 40–100 %, depending on total water column, surface albedo, and viewing geometry. For the region of our study, however, the mean single measurement noise is of the order of 20–50 %, due to the high albedo and optimal viewing geometry of West Africa. This random error can be further reduced by averaging multiple measurements. Therefore, we average the measurements according to the procedure of Yoshimura et al. (2011); we averaged multiple measurements that were collected in a grid of  $2.5^\circ \times 2.5^\circ$  in 6 h. We set the threshold value for averaging to 10, meaning that the average of the SCIAMACHY measurements in every grid cell is based on at least 10 measurements taken within 6 h. From the IsoGSM simulation results, the times of the nearest satellite measurements were extracted (hereafter the process is called “collocation”). Thus, there was no difference in representativeness between the model and the satellite data.

# Interannual variability of isotopic composition in water vapor over West Africa

A. Okazaki et al.

Title Page

Abstract

Introduction

Conclusions

References

Tables

Figures

◀

▶

◀

▶

Back

Close

Full Screen / Esc

Printer-friendly Version

Interactive Discussion



# Interannual variability of isotopic composition in water vapor over West Africa

A. Okazaki et al.

Title Page

Abstract

Introduction

Conclusions

References

Tables

Figures

◀

▶

◀

▶

Back

Close

Full Screen / Esc

Printer-friendly Version

Interactive Discussion



## 2.1.2 In situ measurement of water isotopologues in vapor

To assess the performance of the model at shorter timescales, daily  $\delta^{18}\text{O}_v$  from Tremoy et al. (2012) was used in this study. The  $\delta^{18}\text{O}_v$  was observed at about 8 m above the ground using a Picarro laser instrument (L1102-i model) with an accuracy of  $\pm 0.25\%$  at the Institut des Radio-Isotopes in Niamey, Niger (IRI,  $13.31^\circ\text{N}$   $2.06^\circ\text{E}$ , 218 m.a.s.l.) from 2 July 2010 to 12 May 2011.

## 2.1.3 In situ measurement of isotopes in precipitation (GNIP)

Observations of the monthly isotope ratio in precipitation over West Africa were obtained from the Global Network for Isotopes in Precipitation (GNIP) observational database (IAEA/WMO, 2014). We chose 28 GNIP stations in Africa that have full annual data spanning more than 10 years. The observatory location and its operation period are summarized in Table 1.

## 2.2 Isotope-enabled General Circulation Model simulation

The Isotope-incorporated Global Spectral Model (IsoGSM) is an atmospheric GCM, into which stable water isotopes are incorporated. The model uses T62 horizontal resolution (about 200 km) and 28 vertical levels. The model is spectrally nudged toward wind and temperature fields from the National Centers for Environmental Prediction (NCEP)/Department of Energy (DOE) Reanalysis 2 (R2) (Kanamitsu et al., 2002) in addition to being forced with prescribed SST and sea ice from NCEP analysis. The details of the model configurations were described previously (Yoshimura et al., 2008). The general reproducibility of the model for daily to interannual time scales is well evaluated by comparing with precipitation isotope ratio (Yoshimura et al., 2008) and vapor isotopologue ratio from satellite measurements (Yoshimura et al., 2011), and showed sufficiently accurate results for various process studies (e.g., Berkelhammer et al., 2012; Liu et al., 2013, 2014).

# Interannual variability of isotopic composition in water vapor over West Africa

A. Okazaki et al.

Title Page

Abstract

Introduction

Conclusions

References

Tables

Figures

◀

▶

◀

▶

Back

Close

Full Screen / Esc

Printer-friendly Version

Interactive Discussion



In addition to the standard experiment (Std) mentioned above, we carried out two sensitivity experiments. The first of these experiments examined the sensitivity of the results to the “equilibrium fraction  $\varepsilon$ ,” which is the degree to which falling rain droplets equilibrate with the surroundings. Risi et al. (2010) reported the importance of re-evaporation for  $\delta^{18}\text{O}_v$  over West Africa, and Yoshimura et al. (2011) found an improved simulation result with the changed parameter. Following Yoshimura et al. (2011), we set this value to 10 %, while in the standard simulation it was set to 45 %. The other sensitivity experiment was to estimate the contributions to interannual variability in  $\delta^{18}\text{O}_v$  of the distillation effect during transportation from the source regions. In this experiment, we removed the influences of the distillation processes by turning off isotopic fractionation during condensation and re-evaporation from raindrops and preventing isotopic exchange between falling raindrops and the surrounding vapor. For a similar purpose, Ishizaki et al. (2012) specified transport pathways and then removed these effects along the pathway. We chose a different means of removing the effects in a certain domain, as we wished to specify the area that plays an important role in controlling the isotopic variation at a point. Hereafter, we refer to the former sensitivity experiment as the “E10” experiment and the latter as the “NoFrac” experiment. Std and NoFrac cover the 1979–2012 period, and E10 covers the 2010–2011 period. The simulation results used in this study are basically from Std unless otherwise noted.

We use  $\delta\text{D}$  only when comparing with SCIAMACHY measurements, and  $\delta^{18}\text{O}$  in the other evaluations. As  $\delta\text{D}$  and  $\delta^{18}\text{O}$  basically respond to meteorological factors in the same way, there are no differences in underlying mechanism to produce changes. Therefore, there is no problem using the combination of  $\delta\text{D}$  and  $\delta^{18}\text{O}$  to evaluate model performance.

## 2.3 Isoflux analysis

Isoflux analysis specifies the contributions of advection, evapotranspiration, and precipitation to the changes in isotopic composition of precipitable water in an atmospheric column. The concept of the analysis is based on budget analysis. Using such analysis,

Lai et al. (2006) specifies the factors controlling  $\delta^{18}\text{O}_v$  in a canopy layer. Worden et al. (2007) found the importance of re-evaporation from raindrops. Here, we developed the mass balance equation for  $^{18}\text{O}$  in the atmospheric column. The mass balance for total precipitable water inside the atmospheric column can be written as:

$$\frac{dW}{dt} = -\nabla \cdot Q + E - P \quad (1)$$

where  $W$  represents the total precipitable water,  $Q$  is the vertically integrated two-dimensional vapor flux vector,  $E$  is evapotranspiration, and  $P$  is precipitation. The term  $\nabla \cdot Q$  denotes the horizontal divergence of vapor flux. Here, we refer to this term as advection. A mass balance equation can also be written for  $^{18}\text{O}$  in the same manner as Eq. (1).

$$\frac{dR_W W}{dt} = -\nabla \cdot R_W Q + R_E E - R_P P \quad (2)$$

where  $R_W$ ,  $R_E$ , and  $R_P$  represent the isotope ratio ( $^{18}\text{O}/^{16}\text{O}$ ) of precipitable water, evapotranspiration, and precipitation, respectively. Multiplying Eq. (1) by  $R_W$ , subtracting from Eq. (2) yields:

$$\frac{dR_W}{dt} W = -\nabla R_W \cdot Q + (R_E - R_W)E - (R_P - R_W)P. \quad (3)$$

Dividing by the isotope standard (i.e., VSMOW: Vienna Standard Mean Ocean Water), we can rewrite Eq. (3) in  $\delta$  notation as:

$$\frac{d\delta_W}{dt} W = -\nabla \delta_W \cdot Q + (\delta_E - \delta_W)E - (\delta_P - \delta_W)P. \quad (4)$$

Starting from the left, the terms represent the temporal derivative of the isotopic composition of precipitable water, the effect of advection, evapotranspiration, and precipitation

# Interannual variability of isotopic composition in water vapor over West Africa

A. Okazaki et al.

Title Page

Abstract

Introduction

Conclusions

References

Tables

Figures

◀

▶

◀

▶

Back

Close

Full Screen / Esc

Printer-friendly Version

Interactive Discussion





to deplete or enrich the precipitable water, respectively. As the analysis specifies the contribution of each factor to the change in isotopic composition of precipitable water, the analysis period should start before initiation of isotopic depletion and end at the most depleted point.

### 3 Evaluation of IsoGSM

#### 3.1 Evaluation of IsoGSM at the mean state and seasonal climatology

The annual mean climatology of the SCIAMACHY data and the collocated IsoGSM fields are shown in Fig. 1a and b, respectively. In the SCIAMACHY data, the meridional gradient over West Africa is notable; the lowest values of  $\delta D$  were found in the Sahara and the highest in the Guinea coast. This is due to the dry and therefore HDO-depleted air mass from the subsiding branch of the Hadley circulation in the dry season over the Sahara and strong evaporation and/or recycling of water in the Tropics (Frankenberg et al., 2009). IsoGSM simulates this spatial pattern qualitatively well, but the average is negatively biased (about 20‰) (Yoshimura et al., 2011), and the gradient is weaker in IsoGSM.

Figure 2 shows time–latitude diagrams of  $\delta D$  averaged on 5° W–5° S from 2003 to 2007. Over the region,  $\delta D$  is high in the monsoon season and low in the dry season. In the monsoon season, the isotopically heavy vapor comes from the south along with the monsoon flow. The northern end of the flow coincides with the location of the Inter-Tropical Discontinuity (ITD), which limits the extension of the monsoon flow (Janicot et al., 2008). In the dry season, the subsiding branch of the Hadley cell brings a dry and depleted air mass to the north of the area (Frankenberg et al., 2009). Around 10° N,  $\delta D$  has two minima; one in winter reflecting the depleting effect of subsidence, and the other in summer reflecting the depleting effect of convective activity (Risi et al., 2010). The model captures these two regimes and the depleting effect of convective activity around 10° N in the monsoon season. The correlation between the two figures

Title Page	
Abstract	Introduction
Conclusions	References
Tables	Figures
◀	▶
◀	▶
Back	Close
Full Screen / Esc	
Printer-friendly Version	
Interactive Discussion	



# Interannual variability of isotopic composition in water vapor over West Africa

A. Okazaki et al.

Title Page

Abstract

Introduction

Conclusions

References

Tables

Figures

◀

▶

◀

▶

Back

Close

Full Screen / Esc

Printer-friendly Version

Interactive Discussion



is 0.77 ( $P < 0.001$ ). Note that the range is widely different between them ( $-300$ – $0\%$  for SCIAMACHY;  $-190$ – $90\%$  for IsoGSM). This may be because IsoGSM misses the enrichment in boreal summer over tropical Africa, as suggested in previous studies (Frankenberg et al., 2009; Yoshimura et al., 2011). The bias in the mean field (Risi et al., 2010; Werner et al., 2011; Lee et al., 2012) and underestimated seasonality (Risi et al., 2010) are common to other GCMs. Risi et al. (2010) pointed out the possibility that SCIAMACHY may overestimate the variability by preferentially sampling high altitudes.

Then we compared the simulated  $\delta^{18}\text{O}_v$  with in situ measurement from Tremoy et al. (2012) in Niamey grid point over the 2010–2011 period. Figure 3 shows the time series of near surface daily  $\delta^{18}\text{O}_v$  from the observation and IsoGSM, and the statistics are summarized in Table 2. Note that only the days for which observations were available were used to calculate the statistics. These measurements also showed the two isotopic minima of the year (*W* shape); the first in August and September, and the second in January. The model nicely captures the two minima and simulates well the average and variability, especially in the dry season. On the other hand, the model reveals rather poor reproducibility of day-to-day variation during the monsoon season; the depletion and variability were both overestimated. In the sensitivity experiment E10, the average and standard deviation were comparable with the observation, and the correlation was slightly improved. Although this does not fully explain the discrepancy, it implies that the parameter controlling the equilibrium fraction can be problematic. The positive points are that the  $\delta^{18}\text{O}_v$  and precipitation averaged over previous days showed a strong correlation ( $R < 0.6$ ) southwest of Niamey, as in the observation (Fig. S3 in Tremoy et al., 2012), and the comparable time evolution at the monthly scale (thick lines in Fig. 3). The seasonal differences were similar, suggesting that SCIAMACHY may overestimate the seasonal variability.

## 3.2 Evaluation of IsoGSM at the interannual scale

Finally we evaluate the reproducibility of IsoGSM at the interannual scale. Although our target is surface vapor isotope, we use precipitation isotope to validate the model

reproducibility of surface vapor isotope at the interannual timescale. The reason is twofold; one is the lack of observations of vapor isotope covering several years. The other this is the fact that the isotopic composition of the precipitation is strongly constrained by that of the local lower tropospheric vapor (Risi et al., 2008a). Hence the precipitation isotope somewhat represents surface vapor isotope, and can be used to evaluate the reproducibility of vapor isotope, even though they are not identical.

Figure 4 compares the modeled and observed time series of annual mean  $\delta^{18}\text{O}_p$  at Niamey. Note that there are missing observations from 2000 to 2008, and after 2010. The correlation between them is 0.74 ( $P < 0.05$ ). The simulated (observed) annual average is  $-4.6\text{‰}$  ( $-4.1\text{‰}$ ) and standard deviation is  $1.2\text{‰}$  ( $1.1\text{‰}$ ). The factors controlling the variability will be discussed in Sect. 4.

To summarize the evaluation results, the spatial pattern in the mean state, and the seasonal pattern driven by the Hadley circulation, monsoon flow, and convective activity are qualitatively well simulated with an emphasis on reproducibility of the interannual variability. When compared with SCIAMACHY measurements of  $\delta\text{D}$ , there is a slight bias in the mean state, and IsoGSM largely underestimates the seasonal  $\delta\text{D}$  variations. When compared with the in situ measurements, the bias and variation difference are not as large as when compared with SCIAMACHY. Although the results of the simulation in the monsoon season are not as good as those of the dry season at the daily scale, IsoGSM captures the monthly scale variability fairly well. These results suggest that the model is applicable to study the interannual variability of  $\delta^{18}\text{O}$  during the monsoon season.

## 4 Simulated interannual variability of vapor isotope

### 4.1 General features of interannual variability

In this section, we explore the interannual variability of  $\delta^{18}\text{O}_v$  over Niamey by the standard experiment. The simulation period is from 1979 to 2012. The most striking feature

Title Page

Abstract

Introduction

Conclusions

References

Tables

Figures

◀

▶

◀

▶

Back

Close

Full Screen / Esc

Printer-friendly Version

Interactive Discussion

of the interannual variability is that the depletion in the monsoon season does not appear every year in the model. In contrast,  $\delta^{18}\text{O}_v$  depletion occurs each winter. We term the year with isotopic depletion in the monsoon season the “*W* shape year” following Tremoy et al. (2012). To understand the factors controlling the interannual variability of  $\delta^{18}\text{O}_v$ , it is necessary to investigate the differences between the years with and without depletion. For the purpose of comparison, we set the criteria and made two composite fields: *W* shape year composite and non-*W* shape (*NW* shape) year composite. The quantitative definition of a *W* shape year is a year in which the surface vapor isotope value averaged over JAS in Niamey is  $1\sigma$  (1.1 ‰) less than that of the climatological average (−12.9 ‰). We picked out six *W* shape years (1988, 1999, 2009, 2010, 2011, and 2012) in the period, and the rest are appointed to the *NW* shape composite. The seasonal variations in surface  $\delta^{18}\text{O}_v$  in the two composite fields are shown in Fig. 5.

Here, we briefly discuss the features of the *W* shape years. Figures 6 and 7 show the two composite fields and their differences (*W* shape years minus *NW* shape years) in the monsoon season. *W* shape years are characterized by enhanced monsoon activity; the velocities of southwesterly winds over West Africa are higher (Fig. 6l), and latitudes south of 10° N receive a larger amount of precipitation, especially on the Guinean coast and the West and East Sahel (Fig. 6f). Due to the larger amount of precipitation, the level of evapotranspiration is also higher (Fig. 6i), and hence wetter conditions prevail (Fig. 6c) in *W* shape years. The  $\delta^{18}\text{O}_v$  is more depleted, as expected, centering on Niamey (Fig. 7c). The isotopic compositions of precipitation and evapotranspiration are also more depleted south of Niamey (Fig. 7f and i).

## 4.2 Factors controlling $\delta^{18}\text{O}_v$ at interannual timescales

To identify the mechanism responsible for the difference in isotopic variability between *W* shape and *NW* shape years, isoflux analysis was applied to both composite fields. As the analysis specifies the contribution of each factor to the change in isotopic composition of precipitable water, the analysis period should start before initiation of isotopic depletion and end at the most depleted point. Under this consideration and

# Interannual variability of isotopic composition in water vapor over West Africa

A. Okazaki et al.

Title Page

Abstract

Introduction

Conclusions

References

Tables

Figures

◀

▶

◀

▶

Back

Close

Full Screen / Esc

Printer-friendly Version

Interactive Discussion



because the seasonal variation in the isotopic composition of precipitable water is almost the same as the surface  $\delta^{18}\text{O}_v$  (Fig. 5), the analysis period was June–August to capture the decrease in isotopic composition of precipitable water. We analyzed precipitable water instead of surface vapor for two reasons: first, our simulation does not resolve at what height condensation and re-evaporation take place; and second, most of the atmospheric water resides near the surface, and therefore the isotopic composition of precipitable water may be useful as a proxy for surface  $\delta^{18}\text{O}_v$ .

Figure 8 shows the results for the two composite fields at the Niamey gridcell. First, we discuss how each factor contributes to the  $\delta_W$  variation in general. Precipitation lowers  $\delta_W$ , which is reasonable when considering the Rayleigh distillation model. That is,  $\delta_P$  is greater than  $\delta_W$ ; therefore, the effect of precipitation is always negative, and contributes to lowering  $\delta_W$ . Evapotranspiration works in the opposite way. As the model does not take fractionation into account on the land surface,  $\delta_E$  can be assumed to be a mixture of all precipitation (Yoshimura et al., 2008). Hence,  $\delta_E$  is presumably larger than  $\delta_W$  by the same analogy used to explain the effect of precipitation, and contributes to the increase in  $\delta_W$ . The impact of advection in this form in Eq. (4) seems weaker compared with the other terms. However, the effect of advection in Eq. (4) can be further decomposed into:

$$\nabla \delta_W \cdot Q = \frac{\partial \delta_W}{\partial y} Q_N + \frac{\partial \delta_W}{\partial y} Q_S + \frac{\partial \delta_W}{\partial x} Q_E + \frac{\partial \delta_W}{\partial x} Q_W \quad (5)$$

where  $Q_N$ ,  $Q_S$ ,  $Q_E$ , and  $Q_W$ , represent the vertically integrated two-dimensional vapor flux vector from the north, south, east, and west, respectively. In this form, the impact of advection becomes clearer (Fig. 8b); southerly flow decreases  $\delta_W$ , and easterly flow increases  $\delta_W$ . The impacts of the westerly flow and northerly flow are ambiguous and negligible.

The  $(d\delta_W/dt)W$  is low in  $W$  shape years ( $P < 0.05$ ). Precipitation further lowers  $\delta_W$  and evapotranspiration further increases  $\delta_W$  in  $W$  shape years reflecting the larger amounts of precipitation and evapotranspiration. Although the differences between the

# Interannual variability of isotopic composition in water vapor over West Africa

A. Okazaki et al.

Title Page

Abstract

Introduction

Conclusions

References

Tables

Figures

◀

▶

◀

▶

Back

Close

Full Screen / Esc

Printer-friendly Version

Interactive Discussion



# Interannual variability of isotopic composition in water vapor over West Africa

A. Okazaki et al.

Title Page

Abstract

Introduction

Conclusions

References

Tables

Figures

◀

▶

◀

▶

Back

Close

Full Screen / Esc

Printer-friendly Version

Interactive Discussion



impacts of the two composite fields are large, they are not significant because of the high degree of variation. The only term significantly different other than  $(d\delta_W/dt)W$  is the impact of southerly flow ( $P < 0.05$ ). When regressed with JAS averaged surface  $\delta^{18}\text{O}_v$  at the interannual timescale, the term that shows a strong correlation ( $P < 0.05$ ) is the southerly flow alone. This suggests that the monsoon flow brings depleted moisture produced by heavier precipitation to the Niamey area, controlling the interannual variability of  $\delta^{18}\text{O}_v$ . The interannual regression field of JAS averaged precipitation against Niamey surface  $\delta^{18}\text{O}_v$  shows the correlation at the Guinea Coast ( $10^\circ\text{W}$ – $10^\circ\text{E}$ ,  $\text{EQ}$ – $10^\circ\text{N}$ ; Fig. 9). This indicates the relative importance of the distillation process during transport, as compared to local precipitation for the interannual variability of  $\delta^{18}\text{O}_v$  in West Africa.

In this regard, the correlation between  $\delta^{18}\text{O}_v$  and precipitation east of Niamey, which is also located in the upstream region of Niamey, is expected to be strong, because heavier precipitation falls in the East Sahel in  $W$  shape years and the African Easterly Jet (AEJ) flows toward the Niamey region at heights above 800 hPa. The correlation for this region east of Niamey, however, is relatively weak ( $R < -0.4$ ). As the southerly flow is dominant in the lower atmosphere (1000–800 hPa) in the monsoon season, the relatively weak connection between surface  $\delta^{18}\text{O}_v$  and precipitation east of Niamey is reasonable.

## 4.3 Sensitivity experiment

To confirm the contributions of the amount of precipitation that falls at the Guinea Coast to the interannual variability in  $\delta^{18}\text{O}_v$  at Niamey, we carried out the sensitivity experiment, NoFrac, in which we removed the influence of the distillation process in the Guinea Coast ( $10^\circ\text{W}$ – $10^\circ\text{E}$ ,  $\text{EQ}$ – $10^\circ\text{N}$ ). As shown in Fig. 4, most of the interannual variability in  $\delta^{18}\text{O}_v$  at Niamey was removed. In the standard experiment, the average  $\delta^{18}\text{O}_v$  and the variance at Niamey are  $-12.9\text{‰}$  and 1.16, respectively, whereas they are  $-11.7\text{‰}$  and 0.15, respectively, in NoFrac. The enriched average and considerably

smaller variance in NoFrac confirm the key role of the Guinea Coast precipitation in controlling the interannual variability of  $\delta^{18}\text{O}_v$  at Niamey. In addition, we conducted other sensitivity experiments that were the same as the sensitivity experiment NoFrac but for East Sahel (10–30° E, 10–20° N) and Niamey (10–14° E, 11–15° N). Neither of these experiments showed a significant difference from the standard experiment (data not shown): the average and variance were –12.8‰ (–12.8‰) and 1.07 (1.15), respectively, for East Sahel (Niamey). These results exclude the impact of precipitation in East Sahel or Niamey in controlling the interannual variability, and enhance the robustness of our hypothesis.

## 5 Relationship with ENSO

West African rainfall in the monsoon season has been connected to ENSO (e.g., Janicot et al., 2001; Joly et al., 2007; Losada et al., 2012); i.e., less precipitation during El Niño and more precipitation during La Niña. Given this connection, a relation between  $\delta^{18}\text{O}_v$  and ENSO through precipitation change is expected. Indeed, three of six *W* shape years (1988, 1999, and 2010) fell during a La Niña period. Therefore, we regressed JAS  $\delta^{18}\text{O}_v$  from the model and annually averaged NINO3 index calculated from NCEP SST analysis, which was used to force the model. High positive correlations were found in all of West Africa (Fig. 10a). The spatial distribution of the correlation between the annual average of  $\delta^{18}\text{O}_p$  weighted by monthly precipitation, and the annual averaged NINO3 index was almost identical to the former, but the correlated area over West Africa was confined to south of 15° N (Fig. 10b). To validate this relation, we also show the relation between observed  $\delta^{18}\text{O}_p$  from GNIP and the NINO3 index. The correlation pattern agreed well with GNIP over most of Africa; the highest positive correlation was in West Africa, a weak negative correlation was seen in the south of Central and East Africa, and a weak positive correlation was found in South Africa (Fig. 10c). All of the figures indicate that  $\delta^{18}\text{O}$  is significantly lower (higher) during the cold (warm) phase of ENSO over West Africa. The relation between  $\delta^{18}\text{O}$  in



# Interannual variability of isotopic composition in water vapor over West Africa

A. Okazaki et al.

Title Page

Abstract

Introduction

Conclusions

References

Tables

Figures

◀

▶

◀

▶

Back

Close

Full Screen / Esc

Printer-friendly Version

Interactive Discussion



West Africa and ENSO is evident from the figures. The relation results from the relation between  $\delta^{18}\text{O}$  and West African precipitation, as discussed in Sect. 4, and between the precipitation and ENSO. This mechanism is also found in the Asian and South American monsoon regions: ENSO governs precipitation and the precipitation determines the interannual variability of isotopic composition over the downstream regions (Vuille and Werner, 2005; Ishizaki et al., 2012).

ENSO is not the only mode affecting West African rainfall (Janicot et al., 2001). Therefore, a non-stationary relation between West African rainfall and ENSO (Janicot et al., 1996; Losada et al. 2012) has been reported, but this lies beyond the scope of the present study. Here, we wish to emphasize that we confirmed the statistical relation between rainfall at the Guinea Coast and ENSO, in both observations (Global Precipitation Climatology Project: GPCP, Huffman et al., 2009) ( $R = -0.43$ ,  $P < 0.05$ ) and the model ( $R = -0.45$ ,  $P < 0.05$ ) during the period 1979–2012. Losada et al. (2012) also showed that this relation became significant after the 1970s. Hence, we ensured the robustness of the relation between isotope ratio in surface vapor, precipitation, and ENSO over West Africa.

## 6 Conclusion and perspective

Here, we presented the interannual variability of  $\delta^{18}\text{O}_v$  in West Africa and its relation to ENSO using the nudged IsoGSM model (Yoshimura et al., 2008). Our simulation indicated that the isotopic depletion in the monsoon season, which was reported by Risi et al. (2010) and Tremoy et al. (2012), does not occur every year. The main driver of the depletion was found to be precipitation at the Guinea Coast. Second, we found a relation between  $\delta^{18}\text{O}$  over West Africa and ENSO; ENSO modulates the interannual variability of  $\delta^{18}\text{O}$  via precipitation at the Guinea Coast.

One of the expected roles of isotope-enabled GCM is to find “hot spots”; i.e., places at which a climate proxy is sensitive to climate change, for climate reconstruction. Here, we propose that  $\delta^{18}\text{O}$  at Niamey may be a good proxy of West African rainfall and its



# Interannual variability of isotopic composition in water vapor over West Africa

A. Okazaki et al.

Title Page

Abstract

Introduction

Conclusions

References

Tables

Figures

◀

▶

◀

▶

Back

Close

Full Screen / Esc

Printer-friendly Version

Interactive Discussion



relation to ENSO. Indeed, we found a good correlation between the simulated  $\delta^{18}\text{O}$  and a climate proxy from Ghana, which has a signal of ENSO (Shanahan et al., 2009) for their overlapping period ( $R = 0.65$ ,  $P < 0.01$ ). Despite the strong correlation, however, ENSO is certainly not the single mode modulating  $\delta^{18}\text{O}$  in the area. In our simulation, the last four years were counted as *W* shape years in which surface  $\delta^{18}\text{O}_v$  was lower at Niamey and precipitation over West Africa was higher, even though not all of these were La Niña years. This may reflect the recent La Niña-like trend associated with the hiatus (Kosaka and Xie, 2013; England et al., 2014), supporting the impact of Interdecadal Pacific Oscillation (IPO) on West African rainfall on a multidecadal timescale (Mohino et al., 2011a). On the other hand, Shanahan et al. (2009) reconstructed West African rainfall variability from the sediments of a lake in Ghana, supporting the suggestion that Atlantic SST controls the multidecadal variability. Further comparisons with in situ observations and climate proxies would be of interest.

We showed the ability of the model to simulate intraseasonal to interannual time scale variability, but the model performed relatively poorly on the daily scale. The parameter controlling the equilibrium fraction is suggested to be problematic. Another possibility is the lack of fractionation over the land surface. Risi et al. (2013) demonstrated the importance of continental recycling and sensitivity to model parameters that modulate evapotranspiration over West Africa. They indicated the importance of taking land surface fractionation into account. As IsoGSM assumes that isotopic fractionation does not occur over the land surface, coupling with more sophisticated land surface models would allow more accurate simulations. Similarly, an atmosphere–ocean-coupled model with stable isotopes is desirable to determine how ENSO impacts isotope ratio above water more clearly.

In this study, we did not analyze the interannual variability of the dry season  $\delta^{18}\text{O}$ . However, this dry season  $\delta^{18}\text{O}$  exhibits distinctive variability between *W* shape years and *NW* shape years (Fig. 5). Further studies of the dry season are needed to understand the interannual variability of the hydrological cycle over this area.

*Acknowledgements.* The first author is supported by Japan Society for the Promotion of Science (JSPS) via Grant-in-Aid for JSPS Fellows. A part of this research was supported by the SOUSEI from MEXT, Japan, CREST from JST, Japan, JSPS KAKENHI grant numbers 23686071, 26289160, and the GCOE for Sustainable Urban Regeneration in the University of Tokyo. R. Scheepmaker acknowledges support from the Netherlands Space Office as part of the User Support Programme Space Research project GO-AO/16.

## References

- Aronson, R. B., Precht, W. F., Macintyre, J. G., and Murdoch, T. J. T.: Coral bleach-out in Belize, *Nature*, 405, 36, doi:10.1038/35011132, 2000.
- Berkelhammer, M., Stott, L., Yoshimura, K., Johnson, K., and Sinha, A.: Synoptic and mesoscale controls on the isotopic composition of precipitation in the western US, *Clim. Dynam.*, 38, 433–454, 2012.
- Brown, J., Simmonds, I., and Noone, D.: Modeling  $\delta^{18}\text{O}$  in tropical precipitation and the surface ocean for present-day climate, *J. Geophys. Res.*, 111, D05105, doi:10.1029/2004JD005611, 2006.
- Cai, W., Borlace, S., Lengaigne, M., Rensch, P., Collins, M., Vecchi, G., Timmermann, A., Santoso, A., McPhaden, M. J., Wu, L., England, M. H., Wang, G., Guilyardi, E., and Jin, F.-F.: Increasing frequency of extreme El Niño events due to greenhouse warming, *Nat. Clim. Chang.*, 4, 111–116, doi:10.1038/NCLIMATE2100, 2014.
- Dai, A., Fung, I. Y., Del Genio, A. D.: Surface observed global land precipitation variations during 1900–88, *J. Climate*, 10, 2943–2962, 1997.
- Dansgaard, W.: Stable isotopes in precipitation, *Tellus*, 16, 436–468, 1964.
- England, M. H., McGregor, S., Spence, P., Meehl, G. A., Timmermann, A., Cai, W., Gupta, A., McPhaden, M. J., Purich, A., and Santoso, A.: Recent intensification of wind-driven circulation in the Pacific and the ongoing warming hiatus, *Nature Climate Change*, 4, 222–227, 2014.
- Frankenberg, C., Yoshimura, K., Warneke, T., Aben, I., Butz, A., Deutscher, N., Griffith, D., Hase, F., Notholt, J., Schneider, M., Schrijver, H., and Röckmann, T.: Dynamic processes governing lower-tropospheric HDO/H<sub>2</sub>O ratios as observed from space and ground, *Science*, 325, 1374–1377, 2009.

## Interannual variability of isotopic composition in water vapor over West Africa

A. Okazaki et al.

Title Page

Abstract

Introduction

Conclusions

References

Tables

Figures

◀

▶

◀

▶

Back

Close

Full Screen / Esc

Printer-friendly Version

Interactive Discussion



# Interannual variability of isotopic composition in water vapor over West Africa

A. Okazaki et al.

Title Page

Abstract

Introduction

Conclusions

References

Tables

Figures

◀

▶

◀

▶

Back

Close

Full Screen / Esc

Printer-friendly Version

Interactive Discussion



- Folland, C. K., Palmer, T. N., and Parker, D. E.: Sahel rainfall and worldwide sea temperatures, 1901–85, *Nature*, 320, 602–607, 1986.
- Gianni, A., Saravanan, R., and Chang, P.: Oceanic forcing of Sahel rainfall on interannual to interdecadal time scales, *Science*, 302, 1027–1030, doi:10.1126/science.1089357, 2003.
- 5 Huffman, G. J., Alder, R. F., Bolvin, D. T., and Gu, G.: Improving the global precipitation record: GPCP Version 2.1, *Geophys. Res. Lett.*, 36, L17808, doi:10.1029/2009GL040000, 2009.
- IAEA/WMO: Global Network of Isotopes in Precipitation, The GNIP Database, available at: <http://www.iaea.org/water>, last access: 30 August 2014.
- Ishizaki, Y., Yoshimura, K., Kanae, S., Kimoto, M., Kurita, N., and Oki, T.: Interannual variability of  $\text{H}_2^{18}\text{O}$  in precipitation over the Asian monsoon region, *J. Geophys. Res.*, 117, D16308, doi:10.1029/2011JD015890, 2012.
- 10 Janicot, S., Moron, V., and Fontaine, B.: Sahel droughts and ENSO dynamics, *Geophys. Res. Lett.*, 23, 515–518, 1996.
- Janicot, S., Trzaska, S., and Poccarr, I.: Summer Sahel-ENSO teleconnection and decadal time scale SST variations, *Clim. Dynam.*, 18, 303–320, 2001.
- 15 Janicot, S., Thorncroft, C. D., Ali, A., Asencio, N., Berry, G., Bock, O., Bourles, B., Caniaux, G., Chauvin, F., Deme, A., Kergoat, L., Lafore, J.-P., Lavaysse, C., Lebel, T., Marticorena, B., Mounier, F., Nedelec, P., Redelsperger, J.-L., Ravegnani, F., Reeves, C. E., Roca, R., de Rosnay, P., Schlager, H., Sultan, B., Tomasini, M., Ulanovsky, A., and ACMAD forecasters team: Large-scale overview of the summer monsoon over West Africa during the AMMA field experiment in 2006, *Ann. Geophys.*, 26, 2569–2595, doi:10.5194/angeo-26-2569-2008, 2008.
- 20 Joly, M., Voldoire, A., Douville, H., Terray, P., and Royer, J.-F.: African monsoon teleconnections with tropical SSTs: validation and evolution in a set of IPCC4 simulations, *Clim. Dynam.*, 29, 1–20, 2007.
- 25 Joly, M. and Voldoire, A.: Role of Gulf of Guinea in the interannual variability of the West African monsoon: what do we learn from CMIP3 coupled simulations?, *Int. J. Climatol.*, 30, 1843–1856, 2010.
- Kanamitsu, M., Ebisuzaki, W., Woolen, J., Potter, J., and Fiorino, M.: NCEP-DOE AMIP-II Reanalysis (R-2), *B. Am. Meteorol. Soc.*, 83, 1631–1643, 2002.
- 30 Kosaka, Y. and Xie, S.-P.: Recent global-warming hiatus tied to equatorial Pacific surface cooling, *Nature Climate Change*, 501, 403–407, 2013.

# Interannual variability of isotopic composition in water vapor over West Africa

A. Okazaki et al.

Title Page

Abstract

Introduction

Conclusions

References

Tables

Figures

◀

▶

◀

▶

Back

Close

Full Screen / Esc

Printer-friendly Version

Interactive Discussion



- Lai, C.-T., Ehleringer, J. R., Bond, B. J., and Paw U, K. T.: Contributions of evaporation, isotopic non-steady state transpiration and atmospheric mixing on the  $\delta^{18}\text{O}$  of water vapour in Pacific Northwest coniferous forests, *Plant Cell Environ.*, 29, 77–94, 2006.
- Lamb, P. J.: Large-scale tropical Atlantic surface circulation patterns associated with Subsaharan weather anomalies, *Tellus*, 30, 240–251, 1978.
- Lee, J.-E., Risi, C., Fung, I., Worden, J., Scheepmaker, R. A., Linder, B., and Frankenberg, C.: Asian monsoon hydrometeorology from TES and SCIAMACHY water vapor isotope measurements and LMDZ simulations: implications for speleothem climate record interpretation, *J. Geophys. Res.*, 117, D15112, doi:10.1029/2011JD017133, 2012.
- Liu, G., Kojima, K., Yoshimura, K., Okai, T., Suzuki, A., Oki, T., Siringan, F. P., Yoneda, M., and Kawahata, H.: A model-based test of accuracy of seawater oxygen isotope ratio record derived from a coral dual proxy method at southeastern Luzon Island, the Philippines, *J. Geophys. Res.-Biogeo.*, 118, 853–859, 2013.
- Liu, Z., Yoshimura, K., Bowen, G. J., Buening, N. H., Risi, C., Welker, J. M., and Yuan, F.: Paired oxygen isotope records reveal modern North American atmospheric dynamics during the Holocene, *Nature Communications*, 5, 3701, doi:10.1038/ncomms4701, 2014.
- Losada, T., Rodriguez-Fonseca, B., Mohino, E., Bader, J., Janicot, S., and Mechoso, C. R.: Tropical SST and Sahel rainfall: a non-stationary relationship, *Geophys. Res. Lett.*, 39, L12705, doi:10.1029/2012GL052423, 2012.
- Mohino, E., Janicot, S., Bader, J.: Sahel rainfall and decadal to multi-decadal sea surface temperature variability, *Clim. Dynam.*, 37, 419–440, 2011a.
- Mohino, E., Rodriguez-Fonseca, B., Losada, T., Gervois, S., Janicot, S., Bader, J., Ruti, P., and Chauvin, F.: Changes in the interannual SST-forced signals on West African rainfall, AGCM intercomparison, *Clim. Dynam.*, 37, 1707–1725, 2011b.
- Nicholson, S. E.: The West African Sahel: a review of recent studies on the rainfall regime and its interannual variability, *ISRN Meteorology*, 2013, 1–32, 2013.
- Palmer, T. N.: Influence of the Atlantic, Pacific and Indian Ocean on Sahel rainfall, *Nature*, 322, 251–253, 1986.
- Philander, S. G. H.: Anomalous El Niño of 1982–1983, *Nature*, 305, 16, doi:10.1038/305016a0, 1983.
- Polo, I., Rodriguez-Fonseca, B., Losada, T., and Garcia-Serrano, J.: Tropical Atlantic variability modes (1979–2002), Part I: time-evolving SST modes related to West African rainfall, *J. Climate*, 21, 6457–6475, 2008.

# Interannual variability of isotopic composition in water vapor over West Africa

A. Okazaki et al.

Title Page

Abstract

Introduction

Conclusions

References

Tables

Figures

◀

▶

◀

▶

Back

Close

Full Screen / Esc

Printer-friendly Version

Interactive Discussion



- Risi, C., Bony, S., and Vimeux, F.: Influence of convective processes on the isotopic composition ( $\delta^{18}\text{O}$  and  $\delta\text{D}$ ) of precipitation and water vapor in the tropics: 2. Physical interpretation of the amount effect, *J. Geophys. Res.*, 113, D19306, doi:10.1029/2008JD009943, 2008a.
- Risi, C., Bony, S., Vimeux, F., Descroix, L., Ibrahim, B., Lebreton, E., Mamadou, I., and Sultan, B.: What controls the isotopic composition of the African monsoon precipitation?, Insights from event-based precipitation collected during the 2006 AMMA field campaign, *Geophys. Res. Lett.*, 35, L24808, doi:10.1029/2008GL035920, 2008b.
- Risi, C., Bony, S., Vimeux, F., Frankenberg, C., Noone, D., and Worden, J.: Understanding the Sahelian water budget through the isotopic composition of water vapor and precipitation, *J. Geophys. Res.*, 115, D24110, doi:10.1029/2010JD014690, 2010.
- Risi, C., Noone, D., Frankenberg, C., and Worden, J.: Role of continental recycling in intraseasonal variations of continental moisture as deduced from model simulations and water vapor isotopic measurements, *Water Resour. Res.*, 49, 4136–4156, 2013.
- Rowell, D. P.: The impact of Mediterranean SSTs on the Sahelian rainfall season, *J. Climate*, 16, 849–862, 2003.
- Scheepmaker, R. A., Frankenberg, C., Deutscher, N. M., Schneider, M., Lnadgraf, J., and Aben, I.: Validation of SCIAMACHY HDO/H<sub>2</sub>O measurements using the TCCON and NDACC-MUSICA networks, *Atmos. Meas. Tech.*, in preparation, 2014.
- Schmidt, G. A., LeGrande, A., and Hoffmann, G.: Water isotope expressions of intrinsic and forced variability in a coupled ocean–atmosphere model, *J. Geophys. Res.*, 112, D10103, 2007.
- Shanahan, T. M., Overpeck, J. T., Anchukaitis, K. J., Beck, J. W., Cole, J. E., Dettman, D. L., Peck, J. A., Scholz, C. A., and King, J. W.: Atlantic forcing of persistent drought in West Africa, *Science*, 324, 377–380, 2009.
- Tindall, J. C., Valdes, P. J., and Sime, L. C.: Stable water isotopes in HadCM3: Isotopic signature of El Niño–Southern Oscillation and tropical amount effect, *J. Geophys. Res.*, 114, D04111, doi:10.1029/2008JD010825, 2009.
- Tremoy, G., Vimeux, F., Mayaki, S., Souley, I., Cattani, O., Risi, C., Favreau, G., and Oï, M.: A 1-year long  $\delta^{18}\text{O}$  record of water vapor in Niamey (Niger) reveals insightful atmospheric processes at different timescales, *Geophys. Res. Lett.*, 39, L08805, doi:10.1029/2012GL051298, 2012.

# Interannual variability of isotopic composition in water vapor over West Africa

A. Okazaki et al.

Title Page

Abstract

Introduction

Conclusions

References

Tables

Figures

◀

▶

◀

▶

Back

Close

Full Screen / Esc

Printer-friendly Version

Interactive Discussion



Tremoy, G., Vimeux, F., Soumana, S., Souley, I., Risi, C., Favreau, G., and Oï, M.: Clustering mesoscale convective systems with laser-based water vapor  $\delta^{18}\text{O}$  monitoring in Niamey (Niger), J. Geophys. Res., 119, 5079–5103, doi:10.1002/2013JD020968, 2014.

Vuille, M. and Werner, M.: Stable isotopes in precipitation recording South American summer monsoon and ENSO variability: observations and model results, Clim. Dynam., 25, 401–413, 2005.

Ward, N.: Diagnosis and short-lead time prediction of summer rainfall in tropical North Africa at interannual and multidecadal timescales, J. Climate, 11, 3167–3191, 1998.

Werner, M., Langebroek, P. M., Carlsen, T., Herold, M., and Lohmann, G.: Stable water isotopes in the ECHAM5 general circulation model: toward high-resolution isotope modeling on a global scale, J. Geophys. Res., 116, D15109, doi:10.1029/2011JD015681, 2011.

Worden, J., Noone, D., and Bowman, K.: Importance of rain evaporation and continental convection in the tropical water cycle, Nature, 445, 528–532, 2007.

Yoshimura, K., Kanamitsu, M., Noone, D., and Oki, T.: Historical isotope simulation using Reanalysis atmospheric data, J. Geophys. Res., 113, D19108, doi:10.1029/2008JD010074, 2008.

Yoshimura, K., Frankenberg, C., Lee, J., Kanamitsu, M., Worden, J., and Röckmann, T.: Comparison of an isotopic atmospheric general circulation model with new quasi-global satellite measurements of water vapor isotopologues, J. Geophys. Res., 116, D19118, doi:10.1029/2011JD016035, 2011.

Discussion Paper	Discussion Paper	Discussion Paper	Discussion Paper
------------------	------------------	------------------	------------------

**ACPD**

14, 24441–24474, 2014

---

**Interannual variability  
of isotopic  
composition in water  
vapor over West  
Africa**

A. Okazaki et al.

# Interannual variability of isotopic composition in water vapor over West Africa

A. Okazaki et al.

**Table 2.** Averages, standard deviations, their differences (simulations minus observations) and correlation coefficients for the simulations and observations from the 2010 to 2011 time series.

\*  $P < 0.05$ .

		Ave. [‰]			SD [‰]			Cor.
		Sim.	Obs.	Diff.	Sim.	Obs.	Diff.	
Std	whole period	−14.6	−13.7	0.9	2.2	2.1	0.1	0.46*
	monsoon season	−16.1	−15.2	0.9	2.3	1.8	0.5	0.16
	dry season	−14.7	−15.0	−0.3	1.7	1.6	0.1	0.63*
E10	whole period	−13.9		−0.2	1.7		−0.4	0.46*
	monsoon season	−14.9		−0.3	1.8		0.0	0.20
	dry season	−15.2		−0.2	1.7		0.1	0.64*

Title Page

Abstract

Introduction

Conclusions

References

Tables

Figures

◀

▶

◀

▶

Back

Close

Full Screen / Esc

Printer-friendly Version

Interactive Discussion



# Interannual variability of isotopic composition in water vapor over West Africa

A. Okazaki et al.

Title Page

Abstract

Introduction

Conclusions

References

Tables

Figures

◀

▶

◀

▶

Back

Close

Full Screen / Esc

Printer-friendly Version

Interactive Discussion

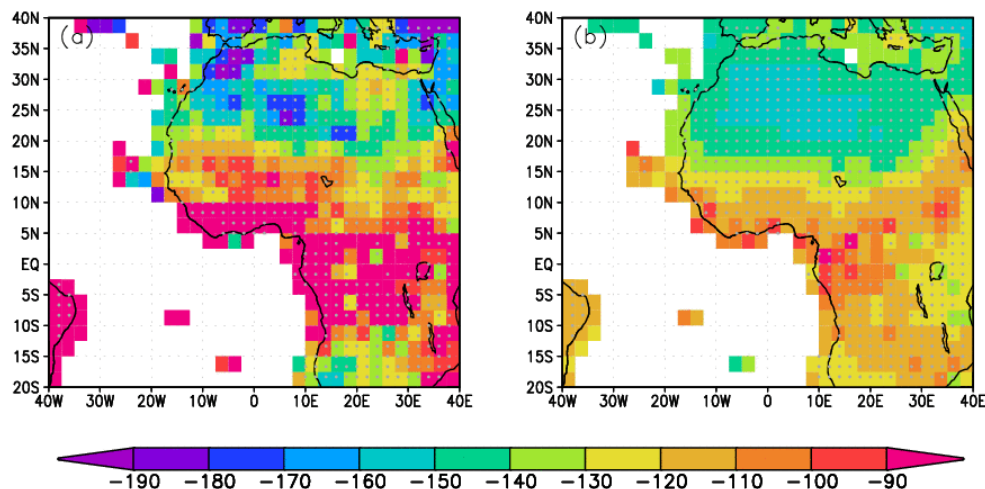


**Figure 1.** Annual mean  $\delta D$  (‰) in column vapor by (a) SCIAMACHY and (b) collocated IsoGSM. Regions in which the measurements did not pass the retrieval criteria were left blank. The shaded grid with dots represents the average of the average, which consists of measurements taken at least 10 times within 6 h.

# Interannual variability of isotopic composition in water vapor over West Africa

A. Okazaki et al.

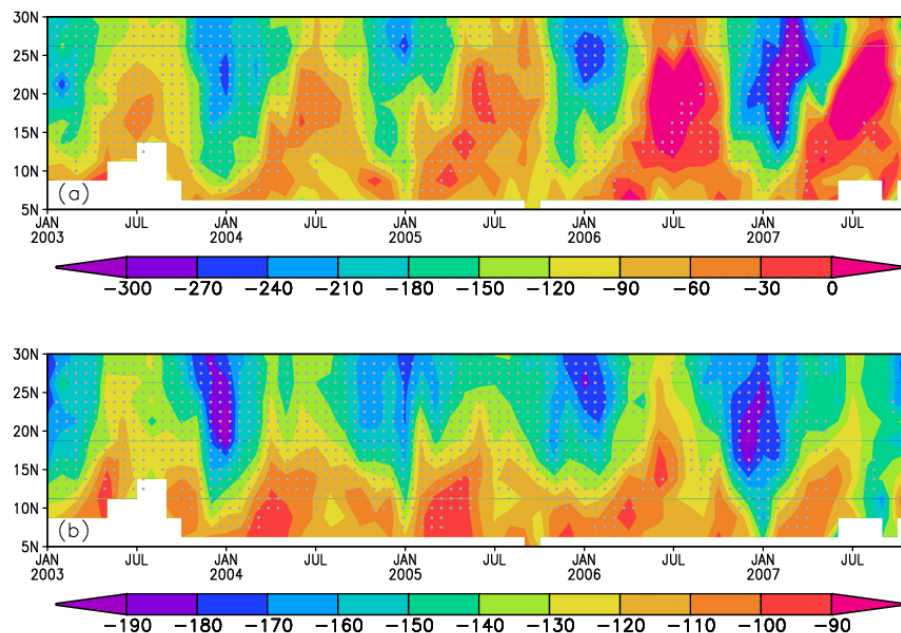


**Figure 2.** Time–latitude diagrams of  $\delta D$  (‰) in column vapor averaged over  $5^{\circ} W$ – $5^{\circ} E$  from 2003 to 2007 by (a) SCIAMACHY and (b) collocated IsoGSM. Regions in which the measurements did not pass the retrieval criteria are left blank. The shaded grid with dots represents the average of the average, which consists of measurements taken at least 10 times within 6 h.

[Title Page](#)[Abstract](#)[Introduction](#)[Conclusions](#)[References](#)[Tables](#)[Figures](#)[◀](#)[▶](#)[◀](#)[▶](#)[Back](#)[Close](#)[Full Screen / Esc](#)[Printer-friendly Version](#)[Interactive Discussion](#)

## Interannual variability of isotopic composition in water vapor over West Africa

A. Okazaki et al.

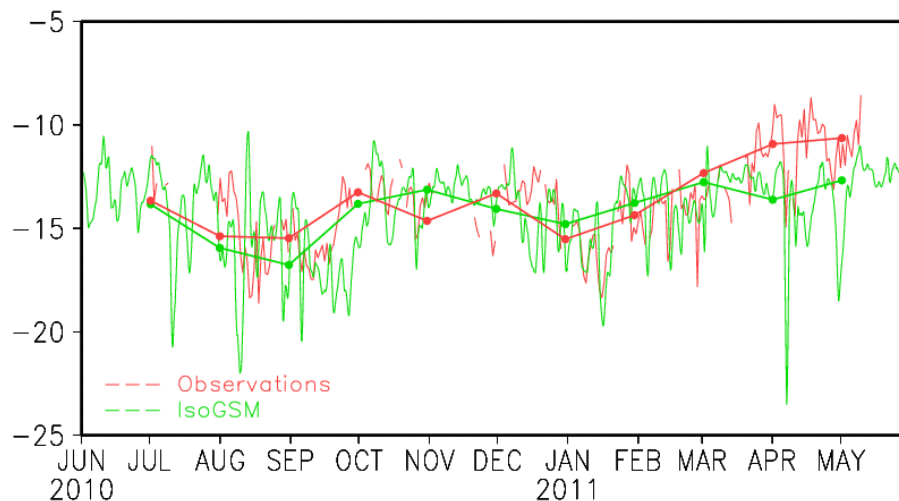


**Figure 3.** Temporal evolution from June 2010 to May 2011 of near-surface  $\delta^{18}\text{O}_v$  (‰): the thin red and green lines are the daily averaged observations and model values, respectively. The thick red and green lines connected by dots are the monthly averaged observations and model values, respectively.

[Title Page](#)[Abstract](#)[Introduction](#)[Conclusions](#)[References](#)[Tables](#)[Figures](#)[◀](#)[▶](#)[◀](#)[▶](#)[Back](#)[Close](#)[Full Screen / Esc](#)[Printer-friendly Version](#)[Interactive Discussion](#)

## Interannual variability of isotopic composition in water vapor over West Africa

A. Okazaki et al.

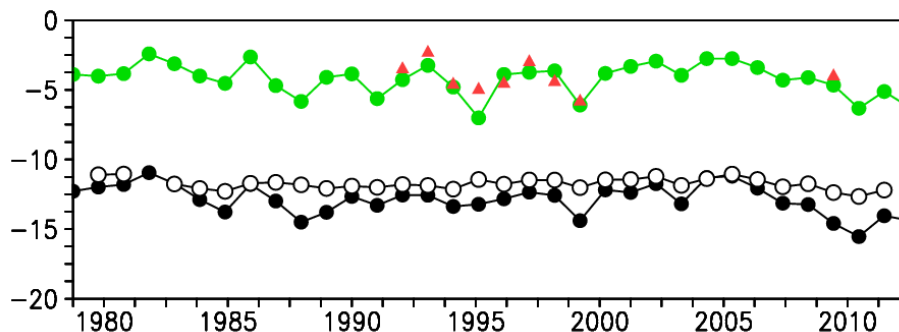


**Figure 4.** Interannual variability of annual mean  $\delta^{18}\text{O}_p$  (‰) at Niamey by the standard experiment (green) and by GNIP observation (red), together with that of near-surface  $\delta^{18}\text{O}_v$  (‰) during JAS at Niamey by the standard experiment (black) and the sensitivity experiment NoFrac (white).

[Title Page](#)[Abstract](#)[Introduction](#)[Conclusions](#)[References](#)[Tables](#)[Figures](#)[◀](#)[▶](#)[◀](#)[▶](#)[Back](#)[Close](#)[Full Screen / Esc](#)[Printer-friendly Version](#)[Interactive Discussion](#)

# Interannual variability of isotopic composition in water vapor over West Africa

A. Okazaki et al.

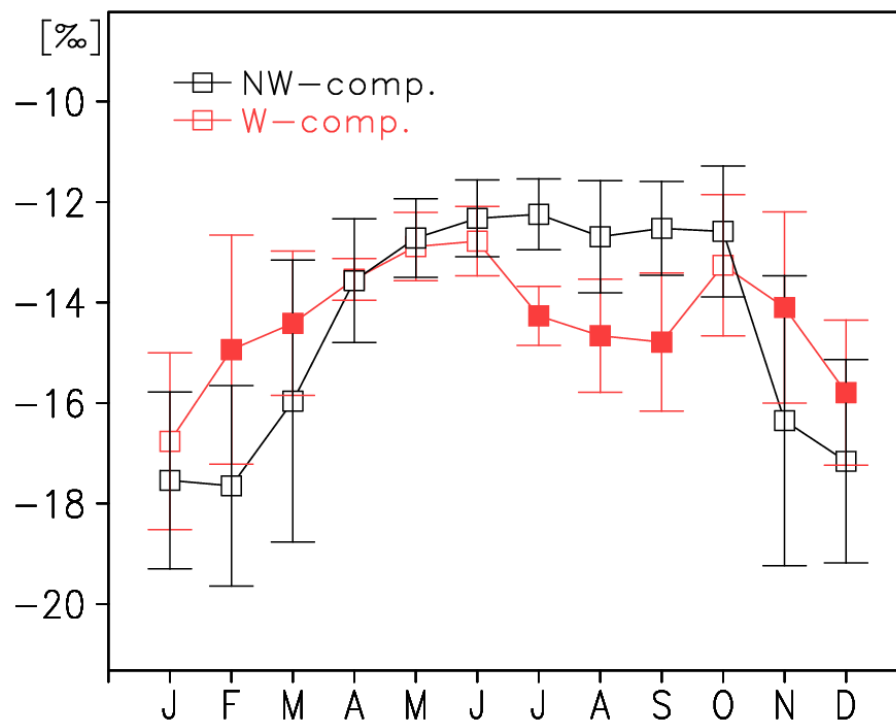


**Figure 5.** Seasonal variation of surface  $\delta^{18}\text{O}_v$  (‰) in *W* shape years (red) and *NW* shape years (black). Bars denote the interannual standard deviations for each month of the two composite fields. Closed red squares indicate that the monthly  $\delta^{18}\text{O}_v$  in the *W* shape year differs significantly from *NW* shape year ( $P < 0.05$ ).

[Title Page](#)
[Abstract](#)
[Introduction](#)
[Conclusions](#)
[References](#)
[Tables](#)
[Figures](#)
[◀](#)
[▶](#)
[◀](#)
[▶](#)
[Back](#)
[Close](#)
[Full Screen / Esc](#)
[Printer-friendly Version](#)
[Interactive Discussion](#)

# Interannual variability of isotopic composition in water vapor over West Africa

A. Okazaki et al.

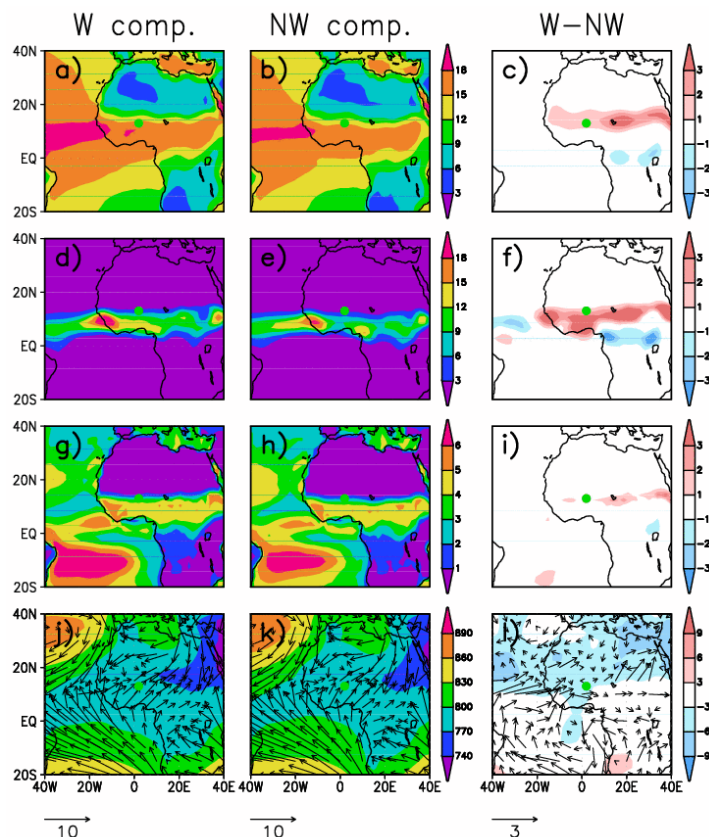


**Figure 6.** JAS average of 2m height specific humidity ( $\text{g kg}^{-1}$ ) (a) in W shape years, (b) in NW shape years, and (c) the difference between them. (d–f) Same as in (a–c) but for precipitation (mm/day). (g–i) Same as in (a–c) but for evapotranspiration (mm/day). (j–l) Same as in (a–c) but for geopotential height at 925 hPa (gpm). Vectors denote wind at 925 hPa.

[Title Page](#)
[Abstract](#)
[Introduction](#)
[Conclusions](#)
[References](#)
[Tables](#)
[Figures](#)
[◀](#)
[▶](#)
[◀](#)
[▶](#)
[Back](#)
[Close](#)
[Full Screen / Esc](#)
[Printer-friendly Version](#)
[Interactive Discussion](#)

# Interannual variability of isotopic composition in water vapor over West Africa

A. Okazaki et al.

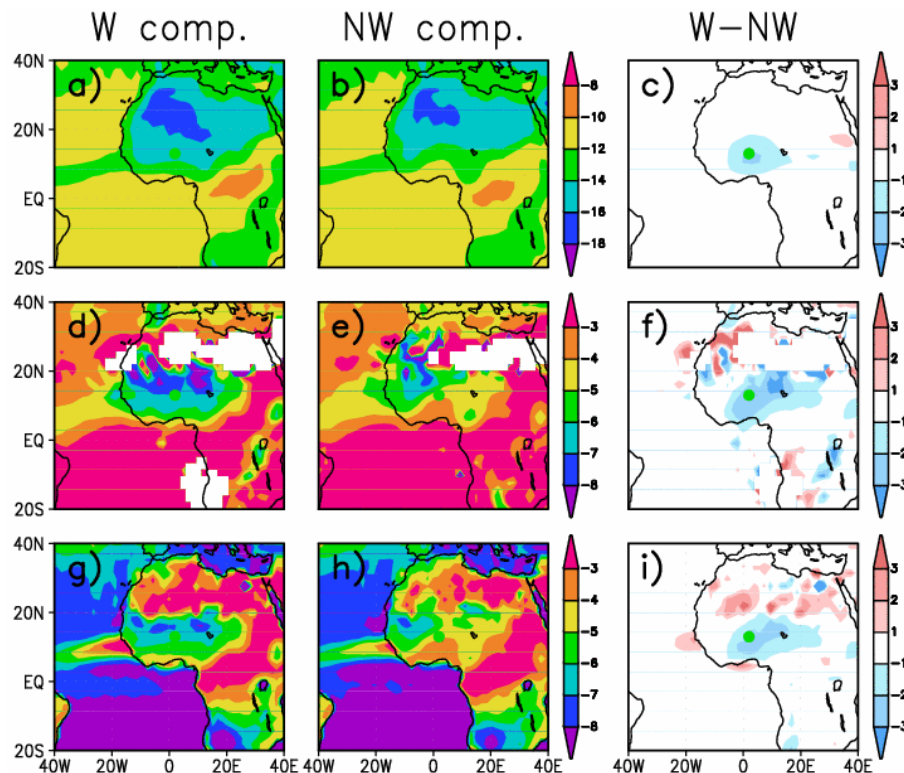


**Figure 7.** JAS average of isotopic composition of 2 m height vapor (‰) **(a)** in *W* shape years, **(b)** in *NW* shape years, and **(c)** the difference between them. **(d–f)** Same as in **(a–c)** but for isotopic composition of precipitation (‰). **(g–i)** Same as in **(a–c)** but for isotopic composition in evapotranspiration (‰).

[Title Page](#)
[Abstract](#)
[Introduction](#)
[Conclusions](#)
[References](#)
[Tables](#)
[Figures](#)
[◀](#)
[▶](#)
[◀](#)
[▶](#)
[Back](#)
[Close](#)
[Full Screen / Esc](#)
[Printer-friendly Version](#)
[Interactive Discussion](#)

# Interannual variability of isotopic composition in water vapor over West Africa

A. Okazaki et al.

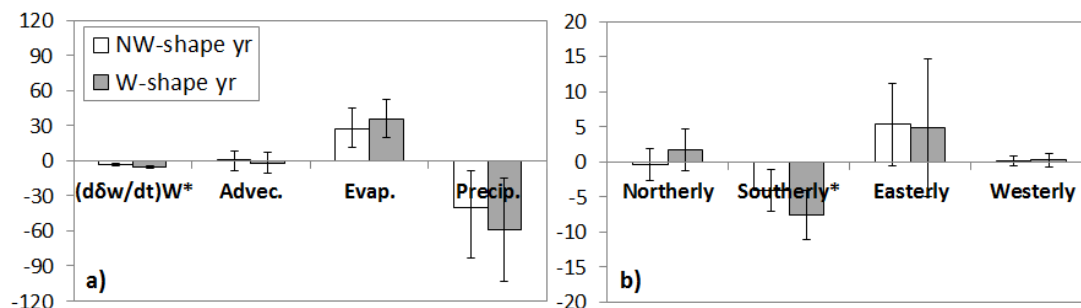


**Figure 8.** (a) Temporal derivative of isotopic composition in precipitable water during JJA and the contributions of advection, evapotranspiration, and precipitation to the vapor isotope change in NW shape years (white) and W shape years (gray) ( $\text{‰ mm day}^{-1}$ ). (b) Same as in (a), but for the decomposed terms of the advection isoflux ( $\text{‰ mm day}^{-1}$ ). \*  $P < 0.05$  between two composites.

[Title Page](#)
[Abstract](#)
[Introduction](#)
[Conclusions](#)
[References](#)
[Tables](#)
[Figures](#)
[◀](#)
[▶](#)
[◀](#)
[▶](#)
[Back](#)
[Close](#)
[Full Screen / Esc](#)
[Printer-friendly Version](#)
[Interactive Discussion](#)



# Interannual variability of isotopic composition in water vapor over West Africa

A. Okazaki et al.

Title Page

Abstract

Introduction

Conclusions

References

Tables

Figures

◀

▶

◀

▶

Back

Close

Full Screen / Esc

Printer-friendly Version

Interactive Discussion

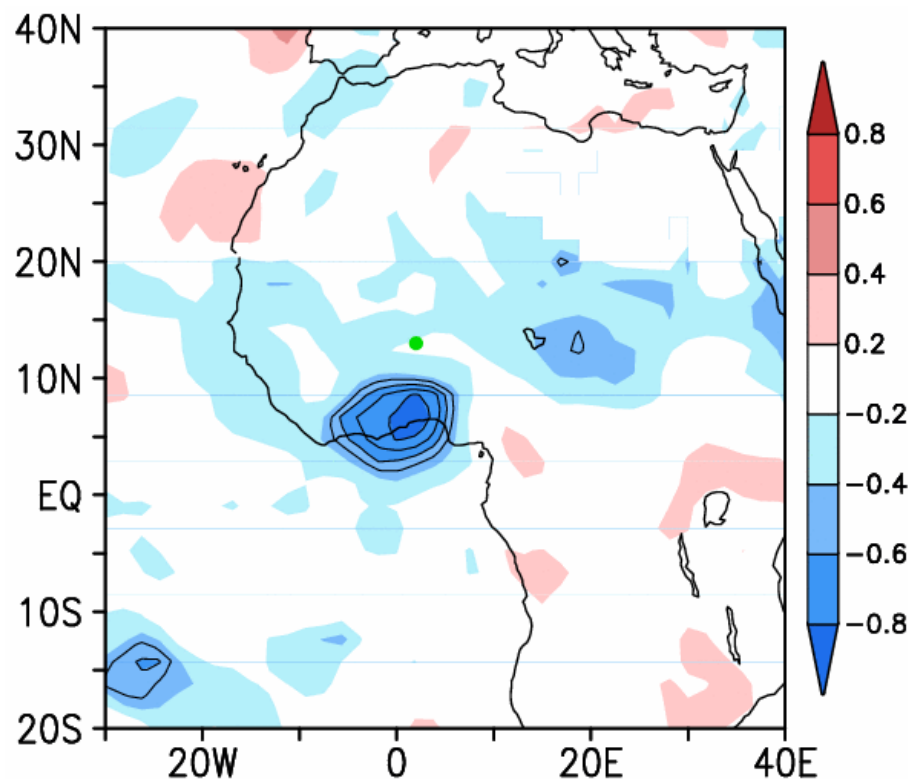


**Figure 9.** Correlation coefficient between JAS averaged  $\delta^{18}\text{O}_v$  at Niamey (green dot) and precipitation. The contoured area represents statistical significance ( $P < 0.01$ ).

# Interannual variability of isotopic composition in water vapor over West Africa

A. Okazaki et al.

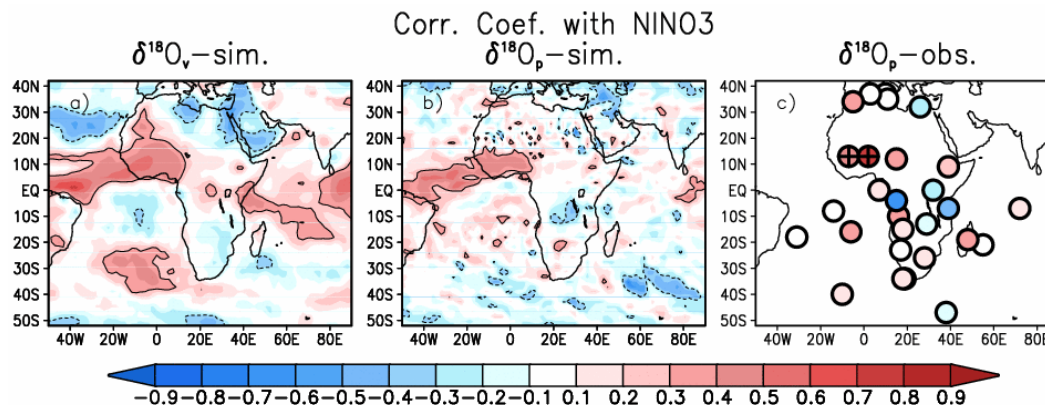


**Figure 10.** Correlation coefficient between annual averaged NINO3 index and (a) simulated July–September averaged vapor isotope, (b) annual averaged simulated precipitation isotope weighted by monthly precipitation, and (c) annual averaged observed precipitation isotope weighted by monthly precipitation. Regions with significant positive (negative) correlations at the 90 % confidence level are circled with solid (dotted) lines in (a) and (b). Sites with significant correlations at the 90 % confidence level are indicated by crosses in (c).

Title Page

Abstract

Introduction

Conclusions

References

Tables

Figures

◀

▶

◀

▶

Back

Close

Full Screen / Esc

Printer-friendly Version

Interactive Discussion